Solubility measurement of methyl anthranilate in supercritical carbon dioxide using dynamic and static equilibrium systems

Wen-Chyan Tsai,* Yonghong Ruan and Syed SH Rizvi
Department of Food Science, Cornell University, 151 Stocking Hall, Ithaca, NY 14853, USA

Abstract: The solubility of methyl anthranilate in supercritical carbon dioxide was determined using dynamic and static equilibrium systems. Three temperatures (40, 60 and 80 °C) and a pressure range between 160 and 340 atm were applied for the dynamic solubility measurements. The flow rate was maintained at 0.5 mL min^{-1} in the dynamic solubility measurements, where the solute solubility was claimed to be independent of the flow-rate factor. Two temperatures (40 and 60 °C) and the pressure range between 100 and 265 atm were used in the static equilibrium system. The crossover pressure region was observed between 220 and 240 atm in the static system, but was not seen in the dynamic system. The solubility of methyl anthranilate determined by the static system was consistently higher than the dynamic solubility measurement, indicating that the static technique provided more reliable solubility data for methyl anthranilate than the dynamic technique. The solubility data obtained with the static system were in good agreement with the predictive models based on the Chrastil equation and the Peng–Robinson equation of state with the Panagiotopoulos and Reid mixing rule.

Keywords: methyl anthranilate; supercritical carbon dioxide; dynamic equilibrium; static equilibrium; solubility

INTRODUCTION

Methyl anthranilate (MA) (methyl 2-aminobenzoate), shown in Fig. 1, is a natural aromatic compound found in grape, citrus and flowers, such as jasmine.[1,2] Under ambient conditions, it is a pale-yellow liquid which possesses a grape-like flavor and a unique bluish fluorescence. It is insoluble in glycerol, slightly soluble in water and soluble in many organic solvents including methanol, acetonitrile and methylene chloride.[3] MA has also been found to have photoprotective activity.[4]

Currently, MA is synthesized and used as a flavor additive in the food industry. A number of commercial MA-added products, such as carbonated or non-carbonated beverages, hard candy, chewing gum, jams and jellies, are commercially available.[3] It is also used as an ultraviolet absorbent in sunscreen products to prevent photo-carcinogenesis.[4] In addition, MA is an effective, non-toxic and non-lethal bird repellent, with application potential for protecting crops, seeds, turf and fish stocks from bird damage.[5]

Carbon dioxide in its supercritical state (>31 °C and >73 atm) has emerged as a viable, environmentally friendly and sustainable alternative solvent for food applications, such as extraction, fractionation, enzymatic reactions and sterilization.[6–10] MA is a non-polar fluorescent flavorant and soluble in supercritical carbon dioxide (SC-CO_2). Reliable solubility data for MA are not available for the design of an efficient MA extraction system with SC-CO_2.

There are two commonly applied methods for measuring a solute's solubility in supercritical fluids (SCFs): a dynamic and a static technique. In the dynamic equilibrium system, an SCF flows continuously through a vessel filled with the solute of interest. The solute-laden fluid then passes a restrictor and is depressurized in a trapping medium for solute recovery. The solubilities of several compounds, e.g. limonene, citral, benzoin, capsaicin and β-carotene, have been reported using this approach.[11–14] In the static equilibrium system, the targeted solute is loaded into an extraction cell connected with a recirculation loop in an insulated environment. An SCF is then introduced into the loop. After recirculation and equilibration, the solute-laden fluid is trapped in a sample loop for recovery and analysis. The solubilities of some compounds, e.g. taxol, sulfamethazine, sulfadimethoxine, dihydroxybenzene and *p*-quinone, have been measured by this technique.[15–18] Although the consistency of solubility measurement by either the dynamic or the static technique is taken for granted, very few comparative evaluations of the two methods have been reported.

In this study, the measurement of the solubility of MA in SC-CO_2 was conducted using the dynamic and static equilibrium systems. The solubility

* Correspondence to: Wen-Chyan Tsai, Department of Food Science, Cornell University, 151 Stocking Hall, Ithaca, NY 14853, USA
E-mail: wt49@cornell.edu
(*Received 16 August 2005; accepted 27 March 2006*)
Published online 3 August 2006; DOI: 10.1002/jsfa.2575

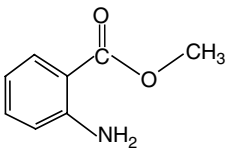

Figure 1. Molecular structure of methyl anthranilate.

data obtained with these two systems were then compared. The correlations of the solubility data were also modeled using the Chrastil equation and the Peng–Robinson equation of state (PR EOS) and compared for their predictability.

MATERIALS AND METHODS

Materials and reagents

Methyl anthranilate ($C_8H_9NO_2$) with a molecular weight of 151.16 was supplied by Acros Organics, Fair Lawn, NJ, USA (purity $>990\,g\,kg^{-1}$). Carbon dioxide (purity $>999\,g\,kg^{-1}$), used as a supercritical solvent, was supplied by Airgas, Ithaca, NY, USA. Table 1 shows some physical properties of MA and CO_2. HPLC-grade hexane (purity $>997\,g\,kg^{-1}$, Fisher Scientific, Fair Lawn, NJ, USA) was used as flushing solvent for sample analyses.

Dynamic solubility measurement

Figure 2 shows a schematic diagram of the dynamic equilibrium apparatus (PrepMaster GA, Suprex Corporation, Pittsburgh, PA, USA) used in this study. It consists of two 10-mL extraction vessels, a varipump system, a pressure transducer, flow control valves and a restrictor. The system temperature was maintained by a temperature-controlled air bath, ranging from 25 to 150 °C. The system pressure (70–550 atm) was controlled by the varipump system. The restrictor temperature can be set between 25 and 150 °C.

Three system temperatures (40, 60 and 80 °C) were applied for solubility measurements at four pressures (160, 220, 280 and 340 atm). The volumetric flow rate was maintained at 0.5 mL min^{-1}, where the solute solubility has been claimed to be independent of the flow-rate factor.[19]

A sample of 2–3 g of liquid MA was loaded in the extraction vessel with clean sea sand. The purposes of stuffing sea sand in the vessel were to prevent physical entrainment of undissolved solute into the saturated

Table 1. Physical properties of MA and carbon dioxide

Substance	Boiling point, T_b (K)	Critical temperature,[a] T_c (K)	Critical pressure,[b] P_c (atm)	Acentric factor,[c] ω
MA	510.2	725.8	35.8	0.577
Carbon dioxide	194.7	304.2	72.8	0.225

[a] Estimated by the Ambrose group contributions.[32]
[b] Estimated by the Ambrose group contributions.[32]
[c] Estimated by the Lee and Kesler equation.[33]

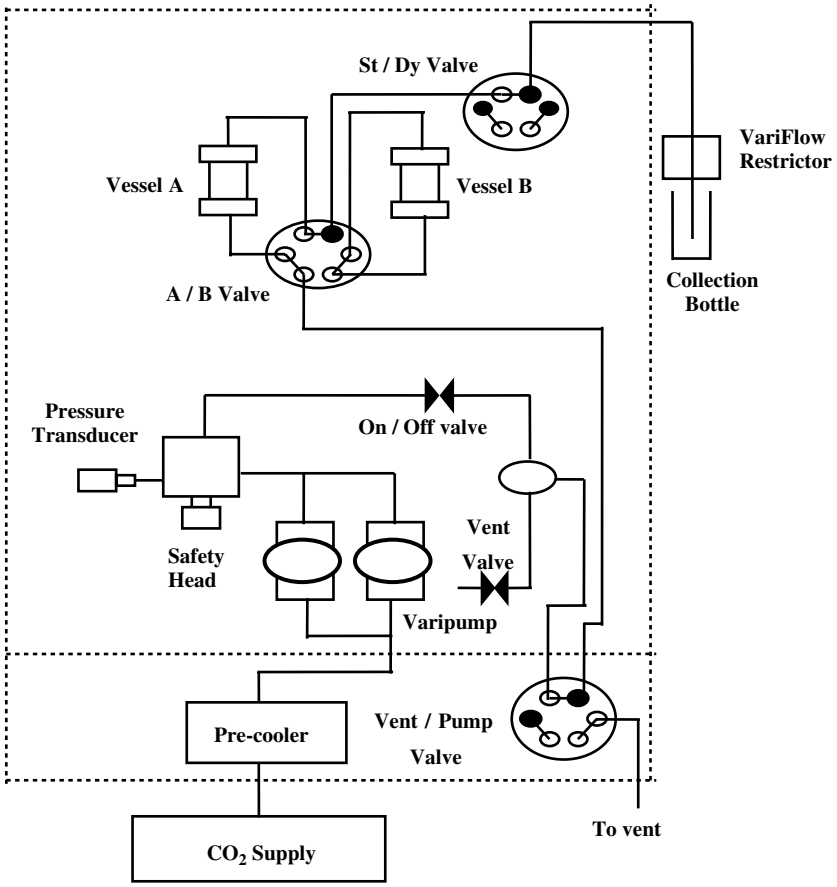

Figure 2. Schematic diagram of the dynamic equilibrium apparatus.

J Sci Food Agric **86**:2083–2091 (2006)
DOI: 10.1002/jsfa

SC-CO_2 and to increase the contact surface between the solute and the solvent. The equilibrium time was set at 10 min followed by 30 min of operation. The restrictor temperature was set at 75 °C to avoid any solute residuals in the tubing. The solute dissolved in SC-CO_2 was collected in the collection bottle at room temperature and pressure and weighed for solubility calculations. The volume and density of the CO_2 used were recorded.

Static solubility measurement

Figure 3 shows a schematic diagram of the static equilibrium system used in this study.[20] The dashed lines set the boundary between the temperature-controlled air bath and the environment. The temperature of the heated enclosure was controlled by proportional controllers (Model 5CX-220P, Oven Industries, Mechanicsburg, PA, USA) and circulation fans (Model 4C549, Dayton Electric, Chicago, IL, USA) to an accuracy of ±0.3 K. The temperatures of the liquid-phase expansion vessel (T1), the system (T2) and the fluid-phase expansion vessel (T3) were measured with resistance temperature devices (RTD, Model 1-PT-100-K-20-15 Ceramic RTD, Omega Engineering, Stamford, CT, USA). The pressures in the view cell (Pv) and the expansion vessels of the vapor and liquid phases (Pe^V and Pe^L) in the system were determined using strain gauge pressure transducers (Model THE-2V3 $0-35 \pm 0.05$ MPa for Pv and Model THE-1V $0-7 \pm 0.02$ MPa for Pe^V and Pe^L; T-Hydronics, Westerville, OH, USA).

Solubility measurements at two temperatures (40 and 60 °C) and pressures in the range between 100 and 265 atm were investigated. Before the experiments were started, the system was flushed several times using HPLC-grade hexane. Next, the system was

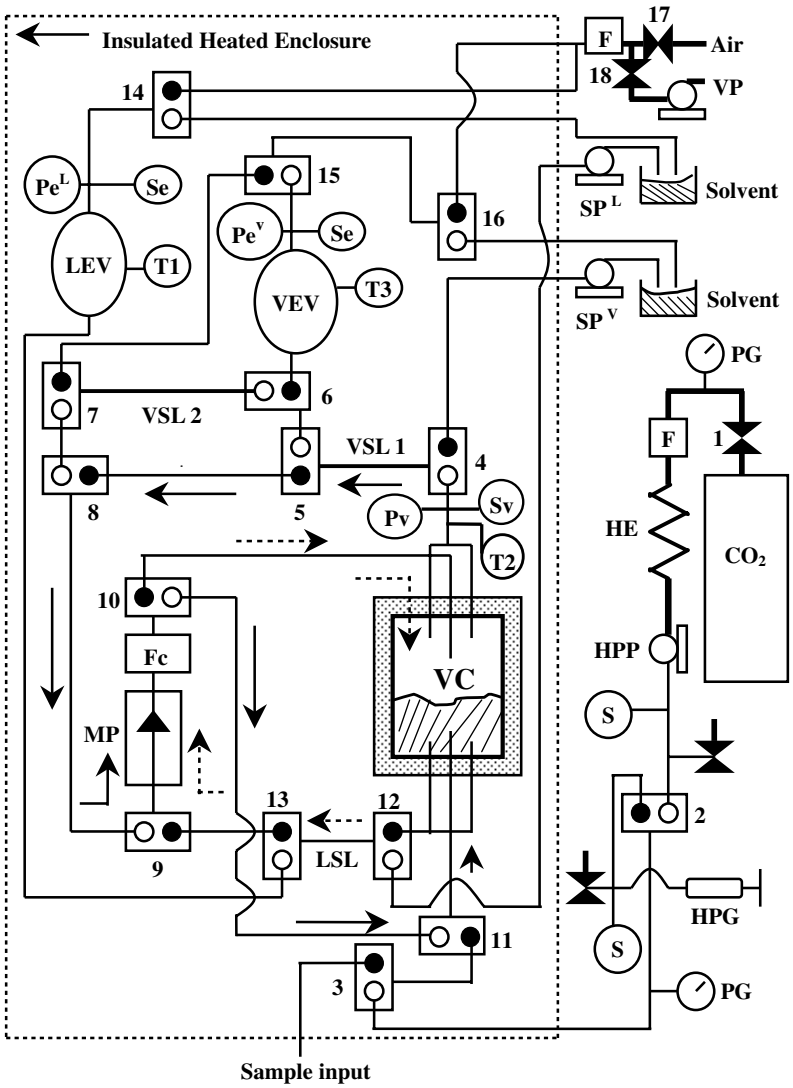

Figure 3. Schematic diagram of the static fluid–liquid equilibrium apparatus. ⊙●, three-way/two-stem combination valve (○, front side; ●, back side); ⧓, two-way straight valve; —, 316 stainless-steel tubing, 3.18 mm o.d., 1.40 mm i.d.; —, 316 stainless-steel tubing, 6.35 mm o.d., 4.57 mm i.d.; HPP, high-pressure pump; MP, magnetic pump; VP, vacuum pump; SP^V and SP^L, solvent pumps for fluid and liquid, respectively; HPG, high-pressure generator; HE, heat exchanger; T1, temperature of liquid-phase expansion vessel; T2, temperature of system; T3, temperature of fluid-phase expansion vessel; Pv, pressure of view cell; PG, pressure gauge; Pe^V and Pe^L, pressures of expansion vessels of fluid and liquid phases, respectively; S, Se and Sv, safety valves; F and Fc, filters; VEV and LEV, expansion vessels of fluid and liquid phases, respectively; VC, view cell; VSL1 and VSL2, fluid sample loops; LSL, liquid sample loop.

dried by air flushing. Then, an adequate vacuum was drawn by a vacuum pump (VP). The head of the high-pressure pump (HPP) was cooled to −5 °C by a chiller.

In the first step, a sample of 15 mL of MA was loaded through valve 3 into the view cell (VC, 50 cm^3), equipped with both front and rear windows. Second, cooled CO_2 was pumped into the view cell by HPP. The pressure level was regulated by a high-pressure generator (HPG). The fluid and liquid phases were recirculated by a magnetic pump (MP). The time of recirculation was set at 1 h to assure that the saturated MA solubility limit was reached.

In this binary phase equilibrium study, the mole fractions of MA in the fluid and liquid phases were determined using sample loops VSL1 and LSL, respectively. The fluid phase recirculated through VSL1 and the by-pass loop between valves 5 and 11 and then back into the view cell, as shown by solid arrows in Fig. 3. The liquid phase passed through LSL and the by-pass loop between valves 9 and 10 and then back into the view cell, as shown by dashed arrows.

Once the recirculation time was completed (1 h), valves 4, 5, 12 and 13 were closed. The samples of the fluid and liquid phases were trapped in VSL1 and LSL, respectively. The trapped sample in VSL1 was expanded into a vapor equilibrium vessel (VEV). Then, the pressure was slowly decreased to atmospheric pressure by releasing CO_2 bubbles through the solvent reservoir. Subsequently, the fluid phase sample (VSL1) was obtained by flushing VEV three times with hexane (125 mL per flushing) using a centrifugal pump (SP^V). The flushed solvents were combined and transferred into a rotary vacuum evaporator to remove the hexane. The trapped sample in LSL was expanded into a liquid equilibrium vessel (LEV), which was followed with the same steps as for the VSL1 sample.

The solvent-removed samples of both phases were rinsed into a weighed aluminum dish (Krackeler Scientific, Albany, NY, USA) with an adequate amount of hexane and then placed in an oven at 40 °C to evaporate the residual solvents. Every 15 min, the samples were weighed gravimetrically until constant weight was reached and then mole fractions of MA were calculated.

Modeling

Generally, two types of mathematical models are used to correlate and to predict a solute's solubility in SCF: statistical methods and equations of state. In this study, the Chrastil equation and PR EOS were applied for each model. The details of these two equations are explained in the following sections. Model comparison was also conducted.

Chrastil[21] developed a semi-empirical correlation to predict a compound's solubility using the solvent density and the reciprocal of operating temperature as independent variables. A linear relationship between a solute's solubility and the solvent density has been reported using this equation:[22–25]

$$\ln C = k \ln \rho + c_1/T + c_0 \tag{1}$$

where C is the solute solubility ($g\,L^{-1}$), ρ the solvent density ($g\,L^{-1}$), T the operating temperature (K) and k, c_1 and c_0 are the equation constants.

Owing to its simplicity and comparative accuracy, PR EOS[26] has been used to predict the phase equilibrium solubilities of liquid or solid solutes in SC-CO_2.[27–30] To extend the range of state from pure fluids to mixtures, the $P-V-T$ relationship in the PR EOS is modified to make the equation parameters composition-dependent, as shown in the following equations:

$$P = RT/(v - b_m) - a_m/[v(v + b_m) + b_m(v - b_m)] \tag{2}$$

$$a_m = \Sigma\Sigma x_i x_j a_{ij} \tag{3}$$

$$b_m = \Sigma x_i b_i \tag{4}$$

$$a = (0.45724R^2T_c^{2/}P_c)\{1 + m[(1 - (T/T_c)^{0.5}]\}^2 \tag{5}$$

$$b = 0.07780RT_c/P_c \tag{6}$$

$$m = 0.37464 + 1.54226\omega - 0.26992\omega^2 \tag{7}$$

where P is the pressure, R the gas constant, T the temperature, v the molar volume, x the mole fraction in the fluid or liquid phases, i and j component identifications, T_c and P_c the critical temperature and critical pressure of a component, ω the acentric factor and a_m, b_m, a, b, a_{ij} and m are the equation parameters.

The cross parameters a_{ij} are related in turn to the pure-component parameters by a mixing rule. The Panagiotopoulos and Reid mixing rule, as shown in Eqn (8), utilizes two interaction parameters to avoid involving too many regression parameters and to improve the accuracy of equations of state:[31]

$$a_{ij} = (a_i a_j)^{0.5}[1 - k_{ij} + (k_{ij} - k_{ji})x_i] \tag{8}$$

where k_{ij} and k_{ji} denote the binary adjustable interaction parameters. The values of the binary interaction parameters (k_{ij} and k_{ji}) were computed using the least-squares method with the fluid and liquid mole fractions as independent variables.

The critical properties were estimated using a group contribution method proposed by Ambrose:[32]

$$T_c = T_b[1 + (1.242 + \Sigma\Delta_T)^{-1}] \tag{9}$$

$$P_c = M_w(0.0339 + \Sigma\Delta_p)^{-2} \tag{10}$$

where T_b is the boiling point (K), M_w the molecular weight and Δ_T and Δ_P are the contributions of different functional groups in a molecule for T_c and P_c.

J Sci Food Agric **86**:2083–2091 (2006)
DOI: 10.1002/jsfa

Owing to a lack of vapor pressure data for MA, its acentric factor (ω) was estimated using the Lee and Kesler equation:[33]

$$\omega = \frac{-\ln P_c - 5.92714 + 6.09648\theta^{-1} + 1.28862\ln\theta - 0.169347\theta^6}{15.2518 - 15.6875\theta^{-1} - 13.4721\ln\theta + 0.43577\theta^6} \quad (11)$$

where $\theta \equiv T_b/T_c$.

To discuss the accuracy of these two models, the goodness of fit was evaluated by the average absolute deviation (AAD):

$$\text{AAD} = \frac{1}{N}\sum_{i=1}^{N}|d_i| \quad (12)$$

where d_i is the difference between the measured and calculated values and N is the number of data points.

Statistical analyses

The solubility variation resulting from different combinations of temperature and pressure was assessed by performing two-way analysis of variance (ANOVA). The results showed no interaction between temperature and pressure. The contributions of both factors were evaluated by applying one-way ANOVA followed by Tukey's procedure, with a significance level of $\alpha = 0.05$. All analyses were conducted using Minitab Release 14 (Minitab, State College, PA, USA).

RESULTS AND DISCUSSION

The MA solubility data at three temperatures (40, 60 and 80 °C) obtained with the dynamic equilibrium system are shown in Table 2. The flow-rate was maintained at 0.5 mL min^{-1} in the dynamic equilibrium system, where the solute solubility was claimed to be independent of the flow-rate factor.[19]

In the pressure range between 160 and 340 atm, the solubility of MA increased significantly with elevation of pressure. When compared at the same pressure, however, the solubility of MA decreased with increase in temperature. Around the lower pressure region, the solubility difference due to temperature was very pronounced. At 160 atm, the solubility of MA at 40 °C was nine times higher than that at 80 °C. Above 220 atm, there was no significant difference between the 40 and 60 °C measurements of the MA solubility. This variation resulting from the change of pressure and temperature was consistent with the solubility measurement of benzoic acid.[34] The solubility of benzoic acid, to which the molecular structure of MA is similar, in SC-CO_2 has also been shown to follow a similar solubility behavior.

Table 3 shows the phase equilibrium data for MA in SC-CO_2 at 40 and 60 °C obtained with the static equilibrium system. Below 220 atm, the MA solubility in the fluid phase at 40 °C was 1.5–2 times higher than that at 60 °C. The solubility of a solute in SCF depends on two major factors: the vapor pressure of the solute, which is exponentially related to the absolute temperature, and the solvating effect of the fluid, which is controlled by its density. With increase in temperature, the solubility loss around the lower pressure region occurs when the solvent density falls, reducing the solvating effect to a greater extent than is made up for by the enhancement of vapor pressure of the solute.

Between 220 and 240 atm, the solubility of MA at 40 and 60 °C was similar, because the vapor pressure enhancement of the solute caused by the increase in temperature counteracts the solubility reduction effect by the solvent's density loss. Therefore, the solubility of the solute at different temperatures may be similar. This phenomenon occurs at the 'crossover pressure' region and has been reported in a number of solubility measurements in SC-CO_2.[35–37] Above this particular pressure, the solubility of the solute increases with increase in temperature.

Table 2. Solubility of MA in SC-CO_2 obtained with the dynamic equilibrium system

	MA (mole fraction)[a,b]		
Pressure (atm)	40 °C	60 °C	80 °C
160	0.0096a,A	0.0028b,A	0.0011bc,A
220	0.0179a,AB	0.0149ab,B	0.0069bc,AB
280	0.0325a,C	0.0307a,C	0.0219b,C
340	0.0559a,D	0.0507a,D	0.0425a,D

[a] $n = 3$.
[b] a–c: Temperature effect. Within a row, different letters denote a significant difference ($P < 0.05$). A–D: Pressure effect. Within a column, different letters denote a significant difference ($P < 0.05$).

Table 3. Experimental fluid–liquid phase equilibrium data obtained with the binary static equilibrium system (SC-CO_2 + methyl anthranilate)

	MA (mole fraction)	
Pressure (atm)	Fluid phase	Liquid phase
40 °C		
100.67	0.0127	0.584
139.06	0.0234	0.446
166.00	0.0293	0.453
172.42	0.0380	0.491
211.79	0.0500	0.256
224.62	0.0454	0.317
228.44	0.0481	0.242
60 °C		
138.07	0.0108	0.396
169.80	0.0204	0.350
175.77	0.0246	0.381
203.95	0.0337	0.318
205.71	0.0304	0.320
235.65	0.0410	0.281
237.89	0.0411	0.291
265.48	0.0742	0.265

Solubility comparison between the dynamic and static equilibrium systems

Figures 4 and 5 show a comparison of the MA solubility measurements in SC-CO_2 between the dynamic and static techniques at 40 and 60 °C, respectively.

In Fig. 4, the solubility obtained using the static equilibrium system at 40 °C is 2–3 times higher than that given by the dynamic system. Owing to the scarcity of MA solubility data, the solubility of a similar compound (methyl *o*-nitrobenzoate[38]) in SC-CO_2 was chosen for comparison. The only difference between these two compounds is that methyl *o*-nitrobenzoate contains a nitro group in place of the amino group in MA. The static solubility of MA in our study is slightly higher than that of methyl *o*-nitrobenzoate. Figure 5 shows that the MA solubility in the static equilibrium system at 60 °C is 2–7 times higher than that in the dynamic equilibrium system.

The dynamic technique, a flow-through design, is a commonly adopted method to determine the solubility of organic compounds in SCFs, because of its simplicity and time efficiency. However, it is sometimes difficult to determine whether the minimum operating flow rate would reach the equilibrium solubility limit or whether the subject solute is being trapped and physically carried over by the flow stream. In contrast, the static technique, a recirculation system, continuously recirculates the SCF through the extractor bed for a prolonged period of time and therefore should provide a more precise measured solubility of a target compound.[35]

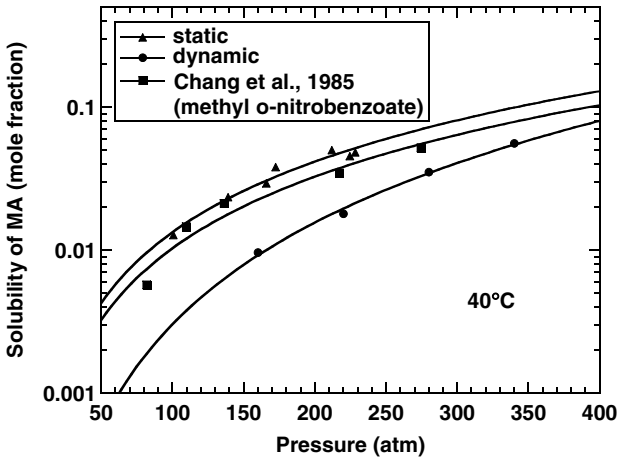

Figure 4. Comparison of solubilities of MA in SC-CO_2 obtained with the dynamic and static systems at 40 °C.

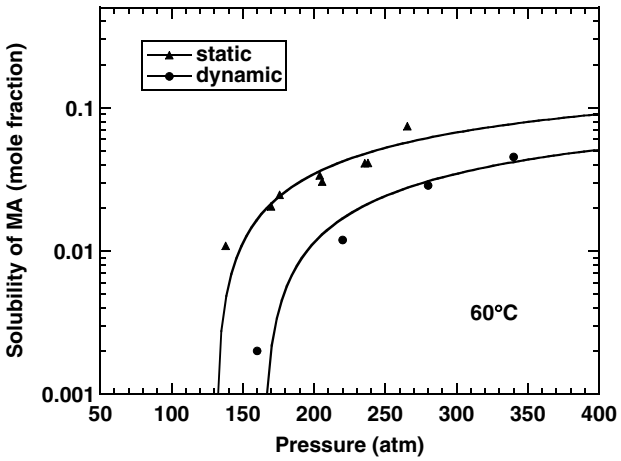

Figure 5. Comparison of solubilities of MA in SC-CO_2 obtained with the dynamic and static systems at 60 °C.

Foster *et al*.[39] reported that the crossover pressure is a phenomenological observation that appears to reflect a property characteristic of the solute and SCF system. Furthermore, it may also be of fundamental significance in providing a direct indicator of the reliability and consistency of experimental solubility data. In the present study, the crossover pressure region was observed around 220–240 atm for the MA solubility measurement using the static equilibrium system, but was not seen in the dynamic equilibrium system. This may suggest that the solubility data of MA in SC-CO_2 obtained with the static technique were more dependable than those with the dynamic technique.

It has been claimed that the dynamic method is an effective, reliable and rapid quantification technique for solubility determination of a solute in SC-CO_2.[40,41] In the present study on MA solubility, the static equilibrium system provided at least two times higher solubility data than the dynamic system, indicating that the equilibrium solubility was not reached in the latter system. MA is highly soluble in SC-CO_2. However, this does not mean that MA would quickly dissolve and equilibrate with SC-CO_2, even when the flow rate is set very low in the dynamic system. The results of this study contest the common practice of using the dynamic technique for solubility measurements. In the following discussion, only the static solubility data were therefore used for development of solubility correlations.

Solubility correlations

Figure 6 shows the correlation of the MA solubility data in the fluid phase from the static system with SC-CO_2 density using the Chrastil equation. This model is based on the assumption that the molecules of a solute associate with the molecules of a fluid to form a solvato complex, which is in equilibrium with the fluid.[21] The points are the experimental solubility data for MA. The dashed and solid lines represent the calculated solubility at 40 and 60 °C, respectively. In terms of natural logarithms, there was a linear relationship between the MA solubility and SC-CO_2 density. The R^2 value was 0.97, which means that the data at 40 and 60 °C were both well correlated with SC-CO_2 density. As for the equation constants, k was 4.8, c_1 was −1165.9 and c_0 was −19.2. In this study, a predictive model of MA solubility in SC-CO_2 was established within the range of temperatures and pressures investigated.

When compared at the same SC-CO_2 density, the solubility of MA at 60 °C was higher than that at

DOI: 10.1002/jsfa

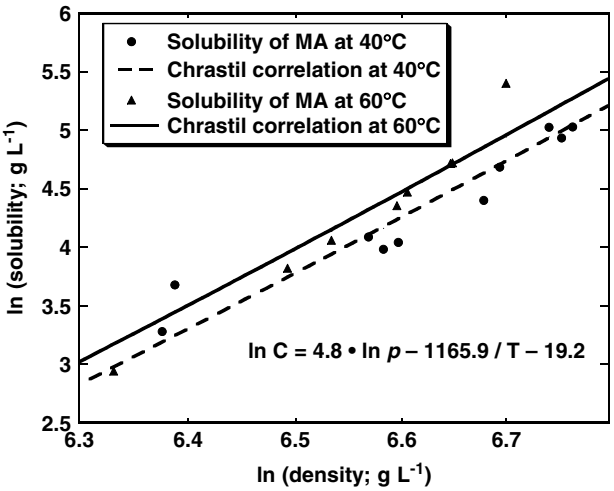

Figure 6. Correlation of the MA solubility data with SC-CO_2 density using the Chrastil equation. Symbols, experimental data; lines, solubility isotherms calculated using the Chrastil equation.

40 °C, as shown in Fig. 6. The temperature effect on the SC-CO_2 density was generalized in this model. In addition, the enhancement of the vapor pressure of MA with increase in temperature allowed more MA molecules to evaporate into the fluid phase. The viscosity of SC-CO_2 also decreased with increase in temperature, which made MA molecules diffuse more easily into the fluid phase. As a result, the higher solubility of MA was determined at higher temperature at the same density of SC-CO_2.

Figures 7 and 8 are the phase diagrams presented as SC-CO_2 mole fractions at 40 and 60 °C, respectively. The diamond and square symbols represent the experimental SC-CO_2 mole fractions in the fluid and liquid phases, respectively, and the solid and dashed lines represent the calculated SC-CO_2 mole fractions in the fluid and liquid phases, respectively.

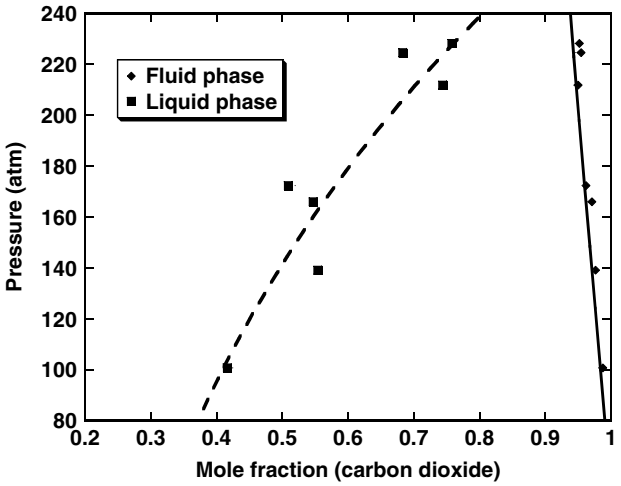

Figure 7. Measured and calculated phase equilibrium solubility for MA and SC-CO_2 in the fluid and liquid phases at 40 °C. Symbols, experimental data; lines, solubility isotherms calculated using the PR EOS with the Panagotopoulos and Reid mixing rule. Solid line, fluid phase; dashed line, liquid phase.

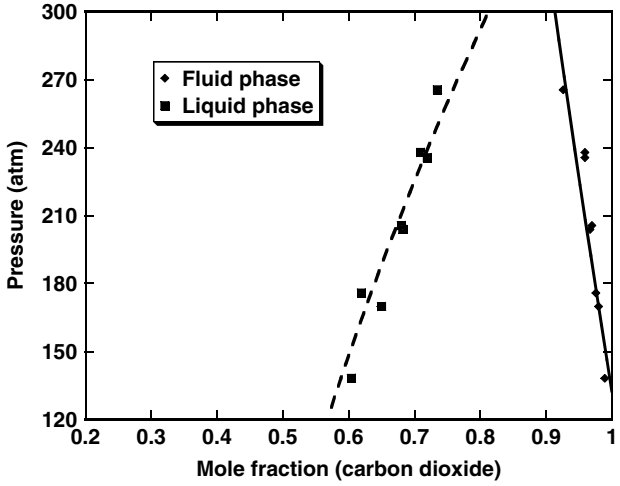

Figure 8. Measured and calculated phase equilibrium solubility for MA and SC-CO_2 in the fluid and liquid phases at 60 °C. Symbols, experimental data; lines, solubility isotherms calculated using the PR EOS with the Panagotopoulos and Reid mixing rule. Solid line, fluid phase; dashed line, liquid phase.

Since the attraction pressure in PR EOS is modified by the molar volume and van der Waals covolume, it is reasonably suited for an asymmetric binary system.[42] Containing two interaction parameters, the Panagiotopoulos and Reid mixing rule was applied to improve the accuracy of computing the fugacity coefficient in the fluid phase using equations of state. It has been shown that this mixing rule provides less correlation deviation when used with PR EOS.[43]

The experimental solubility data were correlated with the critical properties of MA and SC-CO_2 from Table 1 using PR EOS. Because the Panagiotopoulos and Reid mixing rule was applied, two binary interaction parameters (k_{ij} and k_{ji}) were needed. In this study, k_{ij} and k_{ji} were 0.221 and 0.073, respectively. The subscript '*i*' represents SC-CO_2 and '*j*' MA. The goodness of fit was evaluated by computing the average absolute deviation (AAD) and is shown in Table 4. The AAD values were no larger than 0.005, except for the correlation in the fluid phase at 40 °C, which was similar to that reported by Riha and Brunner.[44] The experimental solubility data were well correlated using PR EOS with the Panagiotopoulos and Reid mixing rule. A predictive model was successfully developed.

Table 4. Deviations of the solubility correlations of MA using the Chrastil equation and PR EOS

	AAD[a]			
	40 °C		60 °C	
Method	Fluid	Liquid	Fluid	Liquid
Chrastil equation	0.003	NA[b]	0.004	NA[b]
PR EOS	0.005	0.007	0.003	0.005

[a] AAD $= \frac{1}{N}\sum_{i=1}^{N}|d_i|$.

[b] NA, not available.

In both diagrams, the mole fraction of SC-CO_2 in the fluid phase decreased with increase in pressure, which means that more MA molecules were dissolved in this phase, owing to the stronger solvent power. The mole fraction of SC-CO_2 in the liquid phase increased, which means that more SC-CO_2 molecules were carried into the solute-rich phase. Lee *et al*.[45] proposed that the solubility of SC-CO_2 in the liquid phase increased with increase in pressure, which could be described using the Krichevsky–Ilinskaya (KI) equation and Henry's constant. Similar phase equilibrium phenomena have also been reported by other workers.[44,46]

An open-ended-top saturation loop also exists in both phase equilibria. Hence, for all pressures in the range studied, the fluid and liquid phases coexisted. They may become one homogeneous phase at higher pressure. When these two phase diagrams were compared, the increase in SC-CO_2 mole fraction in the liquid phase at 40 °C was greater than that at 60 °C. At lower temperature, the solubility of SC-CO_2 in the liquid phase was observed to be more sensitive to pressure variations. This implies that a homogeneous phase of SC-CO_2 and MA at 40 °C could be reached at a relatively lower pressure than at 60 °C and was consistent with the findings reported by Brandani *et al*.[37] for the phase behavior of a binary essential oil component and SC-CO_2 system.

Model comparison

Table 4 shows the deviation of the solubility prediction using the Chrastil equation and PR EOS. Because the AAD values of both models are small ($\leq$0.005, except for the correlation of PR EOS in the liquid phase at 40 °C), the solubility correlations with these two models have similar accuracy. The Chrastil equation provides a direct and simple means to predict the solubility of a solute, but it is only a statistical regression and lacks a strong theoretical basis. The solubility correlation by using PR EOS is often more challenging since it requires complex computations and most physical property values are not immediately available in the literature. However, it does provide more theoretical information between equilibrium solubility data and the $P-V-T$ relationships.

CONCLUSIONS

The solubility of MA in SC-CO_2 was more precisely determined by the static than the dynamic technique. The static solubility measurements gave at least two times higher solubility data than the dynamic solubility measurement technique, indicating that equilibrium was not reached in the dynamic system. The equilibrium solubility was reached by recirculation for a prolonged period of time in the static system, which may not be the case with the dynamic system. In addition, the crossover pressure region observed between 220 and 240 atm provided a direct indication of the reliability and consistency of the experimental solubility data obtained with the static system. No crossover pressure region was observed in the dynamic solubility measurement of MA. The results of this study contest the common practice of using the dynamic technique for solubility measurement. Only the static solubility data were therefore used for the development of solubility correlations.

Predictive models based on the Chrastil equation and PR EOS were developed and showed good agreement with the experimental data obtained with the static system. Original and useful information on the solubility of MA in SC-CO_2 is indicative and would economically facilitate the establishment of an up-scaled SC-CO_2 extraction system for functional compounds in essential oils.

ACKNOWLEDGEMENT

The authors thank Dr Rui Hai Liu for use of the equipment in his laboratory in the Department of Food Science, Cornell University.

REFERENCES

1 Lawrence BM, Progress in essential oils. *Perfum Flavor* **22**:45–59 (1997).
2 Ito Y, Sugimoto A, Kakuda T and Kubota K, Identification of potent odorants in Chinese jasmine green tea scented with flowers of *Jasminum sambac*. *J Agric Food Chem* **50**:4878–4884 (2002).
3 Thompson RD and Quaife JT, Liquid chromatographic determination of methyl anthranilate in artificially flavored non-alcoholic beverage. *J AOAC Int* **84**:493–497 (2001).
4 Edlich RF, Winters KL, Lim HW, Cox MJ, Becker DG, Horowitz JH, *et al*, Photoprotection by sunscreens with topical antioxidants and systemic antioxidants to reduce sun exposure. *J Long Term Eff Med Implants* **14**:317–340 (2004).
5 Clark L, Cummings J, Bird S and Aronov E, Acute toxicity of the bird repellent, methyl anthranilate, to fry of *Salmo salar, Oncorhynus mykiss, Ictalurus punctatus* and *Lepomis macrochirus*. *Pestic Sci* **39**:313–317 (1993).
6 Rizvi SSH, Benado AL, Zollweg JA and Daniels JA, Supercritical fluid extraction: fundamental principles and modeling methods. *Food Technol* **40**:55–65 (1986).
7 Arntfield SD, Bulley NR and Crerar WJ, Supercritical CO_2 extraction of egg yolk: impact of temperature and entrainer on residual protein. *J Am Oil Chem Soc* **69**:823–825 (1992).
8 Markom M, Singh H and Hasan M, Supercritical CO_2 fractionation of crude palm oil. *J Supercrit Fluids* **20**:45–53 (2001).
9 Nakaya H, Nakamura K and Miyawaki O, Lipase-catalyzed esterification of stearic acid with ethanol and hydrolysis of ethyl stearate, near the critical portion in supercritical carbon dioxide. *J Am Oil Chem Soc* **79**:23–27 (2002).
10 Ishikawa H, Shimoda M, Shiratsuchi H and Osajima Y, Sterilization of microorganisms by supercritical carbon dioxide micro-bubble method. *Biosci Biotechnol Biochem* **59**:1949–1950 (1995).
11 Giacomo GD, Brandani V, Del Re G and Mucciante V, Solubility of essential oil components in compressed supercritical carbon dioxide. *Fluid Phase Equilib* **52**:405–411 (1989).
12 Cheng KW, Tang M and Chen YP, Solubilities of benzoin, propyl 4-hydroxybenzoate and mandelic acid in supercritical carbon dioxide. *Fluid Phase Equilib* **201**:79–96 (2002).
13 Lee LS, Fu JH and Hsu HL, Solubility of solid 1,4-dimethoxybenzene in supercritical carbon dioxide. *J Chem Eng Data* **45**:358–361 (2000).

14 Hansen BN, Harvey AH, Coelho JAP, Palavra AMF and Bruno TJ, Solubility of capsaicin and β-carotene in supercritical carbon dioxide and in halocarbons. *J Chem Eng Data* **46**:1054–1058 (2001).
15 Nalesnik CA, Hansen BN and Hsu JT, Solubility of pure taxol in supercritical carbon dioxide. *Fluid Phase Equilib* **146**:315–323 (1998).
16 Ashraf-Khorassani M, Combs MT, Taylor LT, Schweighardt FK and Mathias PS, Solubility study of sulfamethazine and sulfadimethoxine in supercritical carbon dioxide, fluoroform and subcritical Freon. *J Chem Eng Data* **42**:636–640 (1997).
17 Yamini Y, Fat'hi MR, Alizadeh N and Shamsipur M, Solubility of dihydroxybenzene isomers in supercritical carbon dioxide. *Fluid Phase Equilib* **152**:299–305 (1998).
18 Coutsikos P, Magoulas K and Tassios D, Solubilities of *p*-quinone and 9,10-anthraquinone in supercritical carbon dioxide. *J Chem Eng Data* **42**:463–466 (1997).
19 Gordillo MD, Blanco MA, Molero A and Martinez de la Ossa E, Solubility of the antibiotic penicillin G in supercritical carbon dioxide. *J Supercrit Fluids* **15**:183–190 (1999).
20 Yu ZR and Rizvi SSH, Phase equilibria of oleic acid, methyl oleate and anhydrous milk fat in supercritical carbon dioxide. *J Supercrit Fluids* **5**:114–122 (1992).
21 Chrastil J, Solubility of solids and liquids in supercritical gases. *J Phys Chem* **86**:3016–3021 (1982).
22 Chen X, Zhao T and Yu W, Solubility measurement of α-asarone in supercritical carbon dioxide. *Fluid Phase Equilib* **211**:11–15 (2003).
23 Subra P, Castellani S, Ksibi H and Garrabos Y, Contribution to the determination of the solubility of β-carotene in supercritical carbon dioxide and nitrous oxide: experimental data and modeling. *Fluid Phase Equilib* **131**:269–286 (1997).
24 Fat'hi MR, Yamini Y, Sharghi H and Shamsipur M, Solubilities of some 1,4-dihydroxy-9,10-anthraquinone derivatives in supercritical carbon dioxide. *J Chem Eng Data* **1998**:400–402 (1998).
25 Murga R, Teresa S, Beltran S and Cabezas JL, Solubility of syringic and vanillic acids in supercritical carbon dioxide. *J Chem Eng Data* **49**:779–782 (2004).
26 Peng DY and Robinson DB, Two-constant equation of state. *Ind Eng Chem Fundam* **15**:59–64 (1976).
27 Huang Z, Lu WD, Kawi S and Chiew YC, Solubility of aspirin in supercritical carbon dioxide with and without acetone. *J Chem Eng Data* **49**:1323–1327 (2004).
28 Abbott AP, Corr S, Durling NE and Hope EG, Solubility of substituted aromatic hydrocarbons in supercritical difluoromethane. *J Chem Eng Data* **47**:900–905 (2002).
29 Vazquez da Silva M and Barbosa D, High-pressure phase equilibrium data for aromatic components of wine: carbon dioxide/*n*-butanal system. *Ind Eng Chem Res* **39**:4427–4430 (2000).
30 Chafer A, Berna A, Monton JB and Mulet A, High pressure solubility data of the system limonene + linalool + CO_2. *J Chem Eng Data* **46**:1145–1148 (2001).
31 Panagiotopoulos AZ and Reid RC, New mixing rule for cubic equations of state for highly polar, asymmetric systems, in *Equations of State: Theories and Applications*, ed. by Chao KC and Robinson JRL. American Chemical Society, Washington, DC, pp. 571–582 (1986).
32 Klincewicz KM and Reid RC, Estimation of critical properties with group contribution methods. *AIChE J* **30**:137–142 (1984).
33 Lee BI and Kesler MG, A generalized thermodynamic correlation based on three-parameter corresponding states. *AIChE J* **21**:510–527 (1975).
34 Schmitt WJ and Reid RC, Solubility of monofunctional organic solids in chemically diverse supercritical fluids. *J Chem Eng Data* **31**:204–212 (1986).
35 Hampson JW, A recirculating equilibrium procedure for determining organic compound solubility in supercritical fluids. Anthracene in carbon dioxide. *J Chem Eng Data* **41**:97–100 (1996).
36 Yamini Y and Bahramifar N, Solubility of polycyclic aromatic hydrocarbons in supercritical carbon dioxide. *J Chem Eng Data* **45**:53–56 (2000).
37 Brandani V, Del Re G, Giacomo GD and Mucciante V, Phase equilibria of essential oil components and supercritical carbon dioxide. *Fluid Phase Equilib* **59**:135–145 (1990).
38 Chang H and Morrell DG, Solubilities of methyl-1-tetralone and methyl nitrobenzoate isomers and their mixtures in supercritical carbon dioxide. *J Chem Eng Data* **30**:74–78 (1985).
39 Foster NR, Gurdial GS, Yun JSL, Liong KK, Tilly KD, Ting SST, *et al*, Significance of the crossover pressure in solid-supercritical fluid phase equilibria. *Ind Eng Chem Res* **30**:1955–1964 (1991).
40 Li Q, Zhang Z, Zhong C, Liu Y and Zhou Q, Solubility of solid solutes in supercritical carbon dioxide with and without cosolvents. *Fluid Phase Equilib* **207**:183–192 (2003).
41 Bristow S, Shekunov BY and York P, Solubility analysis of drug compounds in supercritical carbon dioxide using static and dynamic extraction systems. *Ind Eng Chem Res* **40**:1732–1739 (2001).
42 Yu ZR, Phase equilibria and enzymatic esterification of anhydrous milk fat in supercritical carbon dioxide. PhD Thesis, Department of Food Science, Cornell University, p. 3 (1992).
43 Rodrigues JE, Araujo ME, Azevedo FFM and Machado NT, Phase equilibrium measurements of Brazil nut (*Bertholletia excelsa*) oil in supercritical carbon dioxide. *J Superit Fluids* **34**:223–229 (2005).
44 Riha V and Brunner G, Phase equilibrium of fish oil ethyl esters with supercritical carbon dioxide. *J Supercrit Fluids* **15**:33–50 (1999).
45 Lee MJ, Chen WS and Lin HM, Isothermal vapor–liquid equilibria for binary mixtures of carbon dioxide with hexyl acetate, cyclohexyl acetate or phenyl acetate at elevated pressures. *J Chem Eng Data* **46**:1410–1414 (2001).
46 Bharath R, Yamane S, Inomata H, Adschiri T and Arai K, Phase equilibria of supercritical CO_2–fatty oil component binary systems. *Fluid Phase Equilib* **83**:183–192 (1993).